

High Temperature Ferromagnetism with a Giant Magnetic Moment in Transparent Co-doped $\text{SnO}_{2-\delta}$

S. B. Ogale,^{1,*} R. J. Choudhary,¹ J. P. Buban,² S. E. Lofland,³ S. R. Shinde,¹ S. N. Kale,¹ V. N. Kulkarni,^{1,†} J. Higgins,¹ C. Lanci,³ J. R. Simpson,⁴ N. D. Browning,² S. Das Sarma,⁴ H. D. Drew,⁴ R. L. Greene,¹ and T. Venkatesan¹

¹Center for Superconductivity Research, Department of Physics, University of Maryland, College Park, Maryland 20742-4111, USA

²Department of Physics, University of Illinois at Chicago, 845 West Taylor Street, Chicago, Illinois 60607-7059, USA

³Department of Chemistry and Physics, Rowan University, Glassboro, New Jersey 08028-1701, USA

⁴Department of Physics, University of Maryland, College Park, Maryland 20742-4111, USA

(Received 16 January 2003; published 15 August 2003)

The occurrence of room temperature ferromagnetism is demonstrated in pulsed laser deposited thin films of $\text{Sn}_{1-x}\text{Co}_x\text{O}_{2-\delta}$ ($x < 0.3$). Interestingly, films of $\text{Sn}_{0.95}\text{Co}_{0.05}\text{O}_{2-\delta}$ grown on *R*-plane sapphire not only exhibit ferromagnetism with a Curie temperature close to 650 K, but also a giant magnetic moment of $7.5 \pm 0.5 \mu_B/\text{Co}$, not yet reported in any diluted magnetic semiconductor system. The films are semiconducting and optically highly transparent.

DOI: 10.1103/PhysRevLett.91.077205

PACS numbers: 75.50.Pp, 75.70.-i

Integrating spin functionality into otherwise nonmagnetic solids has become a highly desirable goal in the context of the rapidly developing field of spintronics [1–5] and is of great interest from the fundamental standpoint of structure-chemistry-property relationships in solids. Towards this end, one approach is to introduce magnetic dopants into nonmagnetic solids, and hope that they not only remain magnetically active but also couple with the electronic states of the solid. Considerable success has been achieved in inducing ferromagnetism by transition element doping in compound semiconductor systems [1–4] although the Curie temperatures are much lower than room temperature. In the case of the oxides, the efforts and successes in this context are still relatively limited [6–11] in spite of the fact that many strongly correlated oxides provide interesting grounds for a complex interplay of charge, spin, and orbitals. Early attempts at the synthesis of diluted magnetic semiconductor (DMS) oxides used ZnO as the host and yielded mixed results [6–8]. An indication of favorable results was subsequently obtained in the anatase Co-doped TiO_2 system [9,10], though questions regarding the precise state of cobalt and local microstate of the host are still being sorted out [11].

In this work, we use SnO_2 (rutile) as the host in view of its interesting optical and electrical properties, and widespread applicability [12–16]. While most DMS systems studied thus far are hole doped, SnO_2 (rutile) has *n*-type conduction [17], which is essential for spintronic devices. Mn-doped SnO_2 has been recently explored but no ferromagnetism has been reported [18]. Here we show that Co-doped SnO_2 leads to ferromagnetism with a Curie temperature (T_C) as high as 650 K, still retaining its optical transparency and semiconductivity. Remarkably, at low dopant concentration, a giant magnetic moment of

$7.5 \pm 0.5 \mu_B/\text{Co}$ is also observed, which has not been seen in any DMS system thus far.

The $\text{Sn}_{1-x}\text{Co}_x\text{O}_{2-\delta}$ films were grown by pulsed laser ablation using sintered targets. The substrate temperature, oxygen pressure, laser energy density, and pulse repetition rate were 700 °C, 1×10^{-4} Torr, 1.8 J/cm², and 10 Hz, respectively. The samples were cooled in the same pressure as used during deposition, at the rate of 20 °C/min. It was found that the Co content in the film is considerably higher than that in the corresponding target due to loss of Sn by evaporation. The compositions quoted for the films are therefore the actual concentrations obtained by Rutherford backscattering spectroscopy (RBS). The films were characterized by various techniques.

Figure 1(a) shows the x-ray diffraction (XRD) pattern for a $\text{Sn}_{0.95}\text{Co}_{0.05}\text{O}_{2-\delta}$ thin film grown on *R*-plane sapphire. Only the (101) family of rutile phase film peaks is seen. The rocking curve (inset) full width at half maximum of 0.23° signifies excellent orientational quality. Interestingly, similar good XRD signatures were obtained even for films with Co concentrations as high as 27% ($x = 0.27$). At even higher Co content, a decrease in the XRD intensity was encountered [Fig. 1(b)]. The inset of Fig. 1(b) shows a scanning transmission electron microscopy (STEM) image for a $\text{Sn}_{0.73}\text{Co}_{0.27}\text{O}_{2-\delta}$ film, indicating that even for such high Co content the film microstructure is uniform. Indeed, the electron energy loss spectroscopy (EELS) data recorded at various points spread over the TEM image [Fig. 1(c)] clearly show that cobalt is distributed uniformly in the film. RBS ion channeling data (not shown) exhibited a fairly good channeling for Sn, but hardly any channeling for Co. Since the STEM data do not show any indication of dopant clustering, lack of channeling for Co implies either its interstitial nature or symmetry along a different

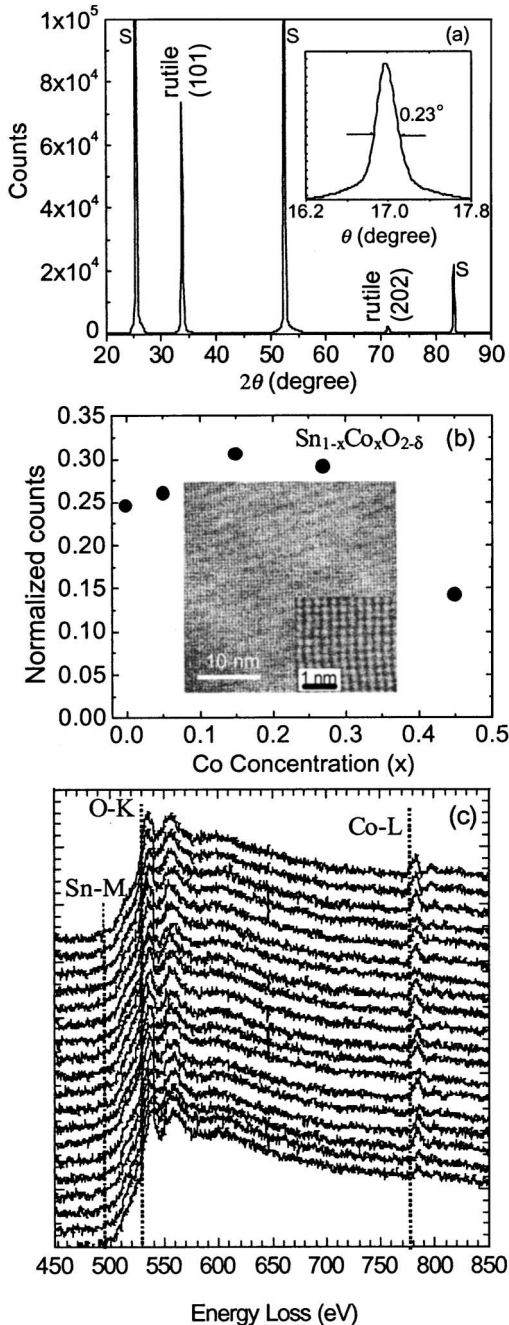


FIG. 1. (a) X-ray diffraction (XRD) pattern for a $\text{Sn}_{0.95}\text{Co}_{0.05}\text{O}_{2-\delta}$ thin film grown on the *R*-plane sapphire substrate. The inset shows the rocking curve (b) normalized (101) XRD peak intensity as a function of the Co content. The inset shows high resolution STEM images for a $\text{Sn}_{0.73}\text{Co}_{0.27}\text{O}_{2-\delta}$ film. (c) EELS data recorded at various points spread over the TEM image domain of the image shown in (b). The spectra show the Sn-M, O-K, and Co-L edges. They are shifted on the *y* scale for clarity.

axis or substitutionality with local distortions leading to an incoherent distribution [19]. The incoherency could arise due to the oxygen vacancy related distortions.

In Fig. 2(a), we show magnetic hysteresis loops at room temperature for $\text{Sn}_{0.95}\text{Co}_{0.05}\text{O}_{2-\delta}$ and $\text{Sn}_{0.73}\text{Co}_{0.27}\text{O}_{2-\delta}$

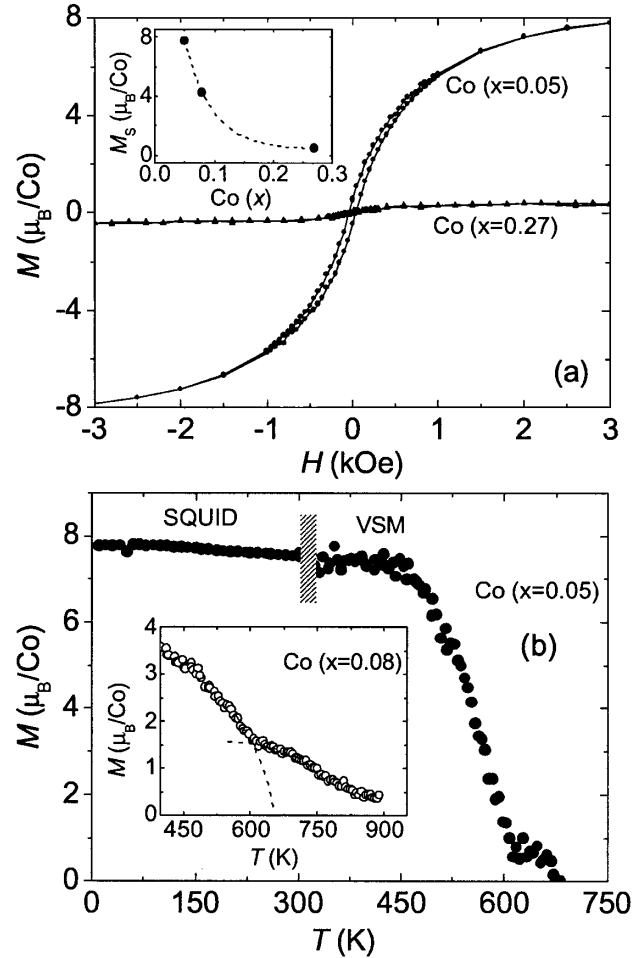


FIG. 2. (a) Magnetic hysteresis loops for $\text{Sn}_{0.95}\text{Co}_{0.05}\text{O}_{2-\delta}$ and $\text{Sn}_{0.73}\text{Co}_{0.27}\text{O}_{2-\delta}$ films at 300 K. The inset shows the dependence of saturation moment M_S on Co concentration x . (b) Magnetization as a function of temperature for the $\text{Sn}_{0.95}\text{Co}_{0.05}\text{O}_{2-\delta}$ film measured from 4.2 to 300 K using SQUID and from 300 to 700 K using VSM. The inset shows the VSM data for the $\text{Sn}_{0.92}\text{Co}_{0.08}\text{O}_{2-\delta}$ film. The dashed lines in the inset are a guide to the eye.

films. A well-defined hysteresis loop with (coercivity ~ 50 Oe) is seen in each case. Remarkably, for the case of the $\text{Sn}_{0.95}\text{Co}_{0.05}\text{O}_{2-\delta}$ film, a giant magnetic moment as high as $7.5 \pm 0.5 \mu_B/\text{Co}$ is observed, and it is seen to drop rapidly with increase in the Co content, as shown in the inset. To our knowledge, no such giant moment has ever been reported in any DMS system. Giant moments have been observed earlier in transition metal doped palladium and alkali metal systems [20–26], and have been a subject of interesting scientific analyses and debate for many years. Realization of such a large moment in an optical material could be useful from the applications standpoint. We will return to the possible origin of such a giant moment and its concentration dependence.

In Fig. 2(b), we show the magnetization (M) as a function of temperature for the $\text{Sn}_{0.95}\text{Co}_{0.05}\text{O}_{2-\delta}$ film measured from 4.2 to 300 K using SQUID and from

300 to 700 K using vibrating sample magnetometry (VSM). M is seen to be fairly constant up to about 475 K, and begins to drop thereafter leading to a T_C close to 650 K. Interestingly, after the sample was cooled to room temperature, M was seen to have dropped by ~ 2.5 . It can thus be inferred that the state of the as-grown film with a giant moment is a metastable one. In the inset of Fig. 2(b), we show the VSM magnetization data for the $\text{Sn}_{0.92}\text{Co}_{0.08}\text{O}_{2-\delta}$ sample. As compared to the $x = 0.05$ Co-doped sample, this $x = 0.08$ sample has a broader tail with nonzero moment extending above 650 K.

In Fig. 3, we compare the optical conductivity for the undoped $\text{SnO}_{2-\delta}$ and $\text{Sn}_{0.73}\text{Co}_{0.27}\text{O}_{2-\delta}$ films. The transparency in the gap region ($\omega < 3.8$ eV) is seen to be virtually unaffected even up to such high Co concentrations. This is illustrated in the inset of Fig. 3. In addition, there is no evidence for impurity levels in the gap as might be expected from the partially filled d states in cobalt. The absorption edge is seen to shift to a higher wavelength (lower energy) for Co-doped sample, indicating matrix incorporation of cobalt atoms. Such shifts are known to occur in DMS systems [27,28].

In Fig. 4(a), we compare the transport properties of the undoped and Co-doped films. While the room temperature resistivity for the undoped film under specified growth conditions is $0.03 \Omega \text{ cm}$, it jumps to about $0.4 \Omega \text{ cm}$ upon $x = 0.05$ Co doping. In films with $x = 0.15$ and $x = 0.27$ Co, the room temperature resistivity is about 200 and $4000 \Omega \text{ cm}$, respectively. Recently, Kilic and Zunger have highlighted a possible key role of the coexistence of Sn interstitials (Sn_i) and oxygen vacancies (V_O) in the unique transport and optical properties of SnO_2 [17]. The surprisingly low formation energies of these defects and their strong mutual attraction are suggested to lead to a natural nonstoichiometry, with the defect stability being attributed to multivalent Sn. With its own multivalent character ($\text{Co}^{3+}/\text{Co}^{2+}$) and small ionic radii, Co ions could favorably compete for interstitial accommodation, thereby forcing Sn_i to their original lattice sites. This (along with the added magnetic scattering) can lead to a rapid rise in resistivity with Co doping, as observed. Indeed, we found a significant drop in carrier concentration upon Co doping, from $\sim 6.55 \times 10^{18}/\text{cm}^3$ in the undoped sample to $\sim 4.45 \times 10^{18}/\text{cm}^3$ in $x = 0.05$ Co-doped film. Also, our RBS data, which did not show any channeling for cobalt, further supports this picture of Co interstitials in a distorted local matrix.

The $\text{Sn}_{0.95}\text{Co}_{0.05}\text{O}_{2-\delta}$ film shows a rapid increase in resistivity below about 10 K presumably due to trapping of the carriers into shallow impurity related traps. This behavior has interesting manifestations in the magnetoresistance [$\text{MR} = (\rho_H - \rho_0)/\rho_0 \times 100\%$, ρ_0 and ρ_H being the resistivity without and with field H], as shown in Fig. 4(b). One can see that the MR is strong and positive at 4 K, while relatively weak and negative at 20 K. At 10 K, it shows a nonmonotonic field dependence. The positive MR at very low temperature which corre-

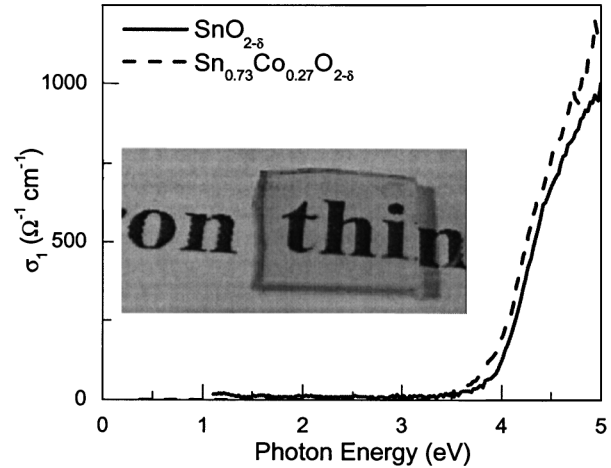


FIG. 3. Optical conductivity (σ_1) in undoped $\text{SnO}_{2-\delta}$ and $\text{Sn}_{0.73}\text{Co}_{0.27}\text{O}_{2-\delta}$ films. The inset shows the transparency of a $\text{Sn}_{0.73}\text{Co}_{0.27}\text{O}_{2-\delta}$ film in the visible range.

sponds to carrier trapping and excitation regime from the shallow traps implies Zeeman splitting of these states due to their strong coupling to the moment of cobalt causing deepening of the traps.

It is now useful to make a few remarks on the giant ($7.5 \pm 0.5 \mu_B/\text{Co}$) magnetic moment observed in the $\text{Sn}_{0.95}\text{Co}_{0.05}\text{O}_{2-\delta}$ film in the as-grown state. This moment is much larger than the value of $\sim 1.67 \mu_B/\text{Co}$ for cobalt metal, or that for small Co clusters ($\sim 2.1 \mu_B/\text{Co}$) [29,30], or that of any of the standard Co oxides wherein the orbital moment is quenched. One possibility is that the atoms surrounding the cobalt atoms have acquired a moment through electronic effects, or the orbital moment of cobalt remains unquenched. Magnetic moments significantly larger ($\sim 6-16 \mu_B/\text{atom}$) than the spin-only moments have indeed been reported in transition metal atoms doped in or spread on the surfaces of alkali metal solids such as Cs [20-26], and these have been attributed to the unquenched orbital contributions. In such cases, an increase in the dopant concentration has been found to cause a rapid decrease in the moment (as observed in our sample) due to enhanced dopant-dopant associations leading to progressive orbital moment quenching. The decreased moment observed in our higher Co-doped samples, and the drop in the moment after a high temperature treatment in low Co-doped sample, possibly caused by enhanced associations, suggest that the scenario may be similar in our case. The tail extending beyond 650 K in the temperature of magnetization for the $x = 0.08$ Co-doped sample also suggests increased dopant association. We observed that argon annealing of a $\text{Sn}_{0.95}\text{Co}_{0.05}\text{O}_{2-\delta}$ film, equivalent to that used in the VSM measurement leading to a drop in the moment, also caused concomitant changes in the transport and structural features. Upon annealing, the resistivity showed an increase [dashed line in Fig. 4(a)], carrier concentration dropped from $\sim 4.45 \times 10^{18}$ to $\sim 3.53 \times 10^{18}/\text{cm}^3$, and

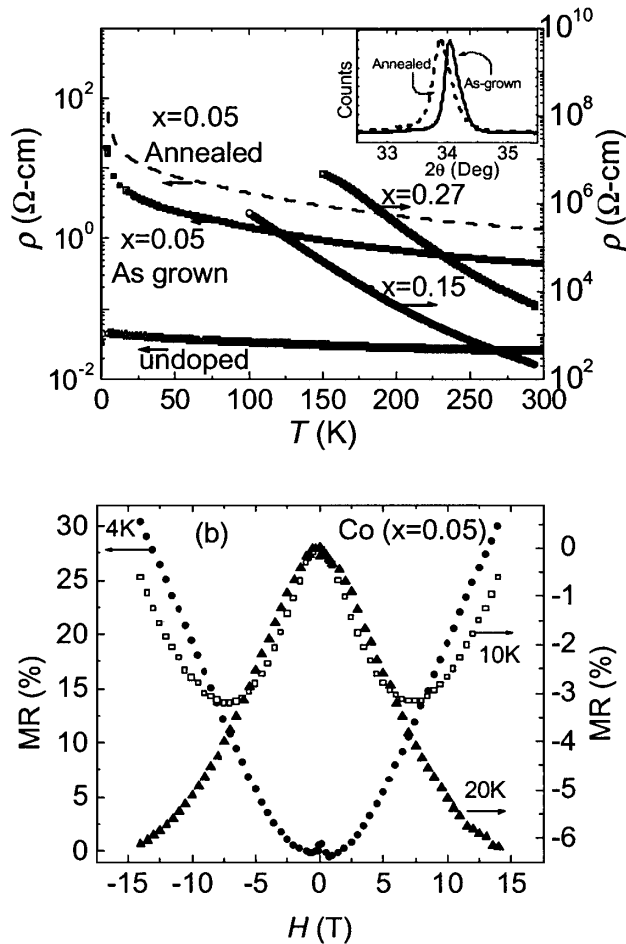


FIG. 4. Temperature dependence of resistivity for the $\text{Sn}_{1-x}\text{Co}_x\text{O}_{2-\delta}$ films; the dashed line shows resistivity for $\text{Sn}_{0.95}\text{Co}_{0.05}\text{O}_{2-\delta}$ film after argon annealing. The inset shows the (101) x-ray diffraction peak for $\text{Sn}_{0.95}\text{Co}_{0.05}\text{O}_{2-\delta}$ film before (solid line) and after (dashed line) annealing. (b) The magnetoresistance (MR) as a function of magnetic field up to 14 T for the $\text{Sn}_{0.95}\text{Co}_{0.05}\text{O}_{2-\delta}$ film at 4, 10, and 20 K.

the (101) lattice parameter relaxed [inset of Fig. 4(a)]. The magnetic moment thus seems to have a close connection with the carrier concentration and the nature of the microstate.

In conclusion, thin films of $\text{Sn}_{0.95}\text{Co}_{0.05}\text{O}_{2-\delta}$ grown by pulsed laser deposition on single crystal sapphire substrates are seen to be ferromagnetic, with a Curie temperature close to 650 K and a giant magnetic moment of $7.5 \pm 0.5 \mu_B/\text{Co}$. Such a giant moment suggests that either the cobalt orbital moment is not quenched or some moment appears on the neighbors of cobalt in the matrix.

The films are highly transparent and semiconducting. No detectable Co clustering is observed in STEM study.

This work is supported by DARPA SpinS program and by NSF-MRSEC (DMR 00-80008) and NSF-ECS-EPDT. The authors would like to thank Chris Lobb and Steven Anlage for critical reading of the manuscript.

*Electronic address: ogale@squid.umd.edu

†On leave from Indian Institute of Technology, Kanpur, India.

- [1] H. Ohno, *Science* **281**, 951 (1998).
- [2] G. A. Prinz, *Science* **282**, 1660 (1998).
- [3] S. A. Wolf *et al.*, *Science* **294**, 1488 (2001).
- [4] Y. D. Park *et al.*, *Science* **295**, 651 (2002).
- [5] S. Das Sarma, *Am. Sci.* **89**, 516 (2001); see also cond-mat/0304219, and references therein.
- [6] T. Fukumura *et al.*, *Appl. Phys. Lett.* **75**, 3366 (1999).
- [7] K. Ando *et al.*, *J. Appl. Phys.* **89**, 7284 (2001).
- [8] K. Ueda, H. Tabata, and T. Kawai, *Appl. Phys. Lett.* **79**, 988 (2001).
- [9] Y. Matsumoto *et al.*, *Science* **291**, 854 (2001).
- [10] S. A. Chambers *et al.*, *Appl. Phys. Lett.* **79**, 3467 (2001).
- [11] S. R. Shinde *et al.*, *Phys. Rev. B* **67**, 115211 (2003).
- [12] M. W. J. Prins *et al.*, *Appl. Phys. Lett.* **68**, 3650 (1996).
- [13] A. V. Tadeev, G. Delabouglise, and M. Labeau, *Thin Solid Films* **337**, 163 (1999).
- [14] E. Comini *et al.*, *Appl. Phys. Lett.* **81**, 1869 (2002).
- [15] J. Y. Kim *et al.*, *Jpn. J. Appl. Phys.* **41**, 237 (2002).
- [16] K. L. Chopra, S. Major, and D. K. Pandya, *Thin Solid Films* **102**, 1 (1983).
- [17] C. Kilic and A. Zunger, *Phys. Rev. Lett.* **88**, 095501 (2002).
- [18] H. Kimura *et al.*, *Appl. Phys. Lett.* **80**, 94 (2002).
- [19] L. E. Depero, P. Levrangi, and G. Sberveglieri, *J. Solid State Chem.* **116**, 256 (1995).
- [20] P. Gambardella *et al.*, *Phys. Rev. Lett.* **88**, 047202 (2002).
- [21] G. Bergmann and M. Hossain, *Phys. Rev. Lett.* **86**, 2138 (2001).
- [22] S. K. Kwon and B. I. Min, *Phys. Rev. Lett.* **84**, 3970 (2000).
- [23] H. Beckmann and G. Bergmann, *Phys. Rev. Lett.* **83**, 2417 (1999).
- [24] Gerd Bergmann, *Phys. Rev. B* **23**, 3805 (1981).
- [25] J. Flouquet *et al.*, *Phys. Rev. Lett.* **38**, 81 (1977).
- [26] R. M. Bozorth *et al.*, *Phys. Rev.* **122**, 1157 (1961).
- [27] Y. D. Kim *et al.*, *Phys. Rev. B* **49**, 1732 (1994).
- [28] Y. D. Kim *et al.*, *Phys. Rev. B* **50**, 10637 (1994).
- [29] J. P. Bucher, D. C. Douglass, and L. A. Bloomfield, *Phys. Rev. Lett.* **66**, 3052 (1991).
- [30] H.-J. Fan, C. Liu, and M. Liao, *Chem. Phys. Lett.* **273**, 353 (1997).